Journal of Applied Mechanics Vol.7,pp.883-890 (August 2004) JSCE

Stability evaluation of fault activity induced by CO_2 injection into deep saline aquifers

CO_2地中貯留における断層の安定性に関する評価研究

Qi Li[1], Zhishen Wu[2] and Xiaochun Li[3]
李 琦・呉 智深・李 小春

[1] Dr. of Eng., Dept. of Urban & Civil Eng., Ibaraki University
(4-12-1, Nakanarusawa-cho, Hitachi, Ibaraki 316-8511, Japan)
[2] Dr. of Eng., Professor, Dept. of Urban & Civil Eng., Ibaraki University
(4-12-1, Nakanarusawa-cho, Hitachi, Ibaraki 316-8511, Japan)
[3] Dr. of Eng., Research Institute of Innovative Technology for the Earth
(9-2 Kizugawadai, Kizu-cho, Soraku-gun, Kyoto 619-0292, Japan)

Carbon dioxide (CO_2) sequestration offers an attractive opportunity for reducing the greenhouse gas emission on our planet. Geological sequestration in deep saline aquifers is widely regarded as a reasonable option for long-term disposals of captured CO_2 in the future. In this paper, we firstly present a numerical model to consider effects of the pore pressure on fault activity. Then, the shear stress and relative slip along the fault surface under different dip angles are compared with or without considering the pore pressure. Finally, the slip tendency and the local safety factor of the faults are evaluated to quantitatively assess the influence of the pore pressure induced by CO_2 injection into deep saline aquifers. From our research, the shear stress change of fault surfaces induced by the pore pressure is clear, and the effects of the pore pressure on the fault surfaces are sensitive to the dip angles of the faults.

Key Words: CO_2 injection, fault, pore pressure, slip tendency, safety factor

1. Introduction

Japan's strategies for the safe underground storage of carbon dioxide in porous geomedia are being developed in the NEDO (New Energy and Industrial Technology Development Organization) research program. Large volumes of CO_2 may be geologically stored by injecting supercritical and thus pressurized CO_2 into saline aquifers or depleted hydrocarbon reservoirs and fields. Injection requires displacement or compression of existing formation fluid, thus injection needs to be at pressures above that of the prevailing fluid. Increasing formation pressures due to CO_2 injection can potentially open fractures and cause slip on faults that exist in a reservoir. This would create or enhance fracture permeability while the formation of networks of interlinked open fractures and rough fault surfaces could provide conduits for the escape of CO_2-rich fluid from a reservoir or a saline aquifer. The NEDO research program is undertaking geomechanical modelling in order to avoid induced fracturing and unwanted fluid migration at any potential CO_2 injection sites. A primary goal of the geomechancial modelling is to estimate the maximum sustainable formation pressures that will not reactivate existing faults or induce new fractures.

Estimates of the fluid pressures that can induce slip on pre-existing faults require knowledge of in situ stresses, fault orientations, fault frictional properties, and prevailing fluid pressures. The determination of such input parameters is thus a prerequisite for the geomechanical modelling of maximum sustainable formation pressures in potential CO_2 storage sites. In addition, geomechanical modelling demonstrates that stress changes induced by pore pressure depletion in

depleted hydrocarbon reservoirs and fields need to be determined prior to any CO_2 injection because these changes will affect the fault slip tendency.

Although many researches have been done on the topic of CO_2 sequestration in the past, there are few researchers to consider influences of the pore pressure induced by the injection on the stability evaluation of faults. In this paper, we first present a geomechanical model to consider effects of the pore pressure on fault activity. Then, the shear stress and relative slip along the fault surface under different dip angles are compared with or without considering the pore pressure. Finally, the slip tendency and the local safety factor are evaluated to quantitatively assess the influence of the pore pressure induced by the injected CO_2 bubble on the faults.

2. Model Description

In this paper, a typical two dimensional model with a plane strain assumption is considered. This model is focused to evaluate the pore pressure effect on faults in our process of developing a strong assessment methodology on fault activity induced by the injected CO_2 bubble, so one part of the initial structural model, which is discussed in our previous work [5] [6], is taken into account, shown in Fig. 1. The finite element mesh of the fault model with a dip angle of 60 degrees is shown in Fig.2. The main material parameters used in our study are listed in Table 1. The fault is embedded into the numerical simulation model according to Fig.1, and two typical fault cases, NA and FB, near and far from the CO_2 bubble, are considered, which is listed in Table 2.

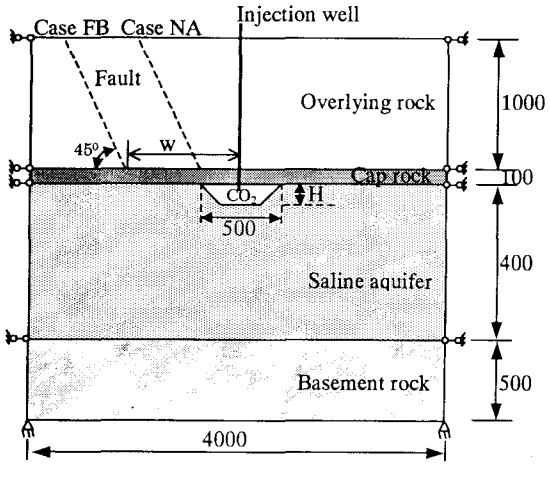

Fig. 1 The sketch of geomechanical model (unit: m)

In our research, one classic method named flexible joint element method to solve contact problems, such as faults, is introduced, which is regarded as being suitable for simulating small slip, small deformation and the arbitrary contact surface meshing. The fault modeling can be depicted in the plot of Fig.3. On the fault surfaces, the same normal stiffness 2.0E+7 Pa/m and shear stiffness 1.0E+7 Pa/m are supposed to use in our research.

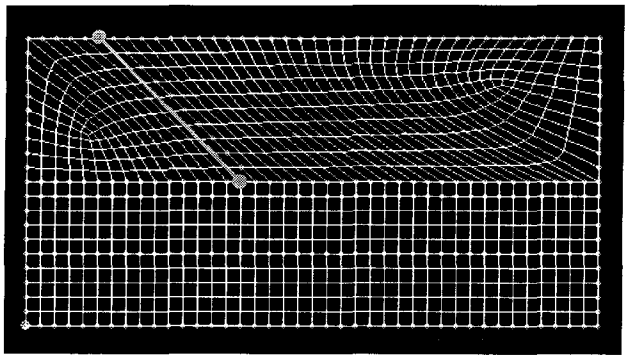

Fig.2 Finite element mesh

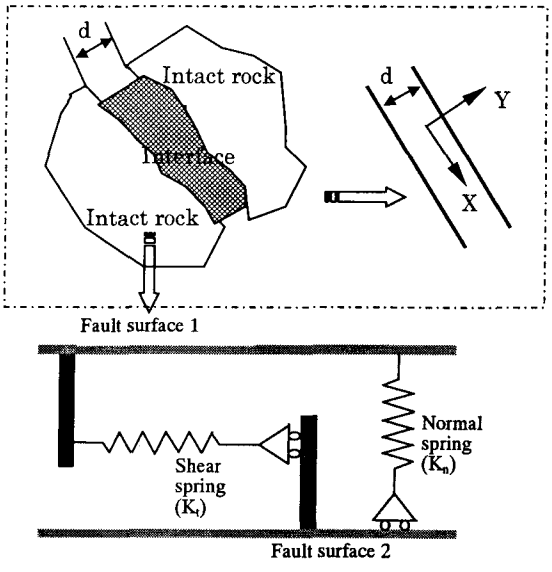

Fig.3 Modeling and local coordinate for fault interfaces

Table 1 Properties of geological materials

Material	Young's Modulus (Pa)	Poisson's ratio	Density (kg/m^3)	Permeability (m/s)
Overlying rock	1.0E+09	0.25	1900	1.0E-7
Cap rock	2.0E+09	0.25	1900	1.E-11
Saline aquifer	2.0E+09	0.25	1900	1.E-6
Basement rock	1.0E+10	0.25	2600	1.E-11

Table 2 Fault cases

Fault case	W (m)
NA	250
FB	500

Note: W is the distance from the center of the CO_2 bubble to the bottom end of the fault.

3. Procedures of Simulation

The basic steps in our numerical simulation are as follows:

Step 1: To finish the equilibrium of the geological initial stress by applying the gravity.

Step 2: To process the transient consolidation process during the initial CO_2 injection stage.

Step 3: To apply the injected CO_2 bubble driven buoyancy to elements of the CO_2 occupied zone as surface distributed force loads.

Step 4: To simulate the variation of stress and deformation of the fault model and compare with the results of the model without considering the pore water pressure.

4. Discussion of Numerical Results

4.1 Variation of Shear Stress and Distribution of Pore Pressure

Normally, the processed CO_2 is injected into 800m deep aquifers and the injected CO_2 is supercritical under such a depth level. In this paper, the depth, 1100m, of the injection well is adopted in order to consider the first geological sequestration project started at the Iwanohara Base of the Teikoku Oil Co. Ltd. in Nagaoka city, Niigata prefecture, Japan. Because the injection always leads to the change of the pore pressure in the sequestration formation layers, and this change has an obvious influence on the fractured zone around the disposal site. In our research, at first, the shear stress variation along the fault surface has been compared under the consideration or non-consideration of the pore pressure in the model. Then, effects of the injected CO_2 volume, i.e. the size of CO_2 bubble, on the variation of shear stress along the fault surface are discussed.

Fig. 4 shows the shear stress change of fault Case NA under the different disposal thickness, H from 100m to 250m, of the CO_2 bubble without considering the pore pressure in the model. H100w/oPor in Fig.4 means that the calculation is under the condition of CO_2 disposal thickness H=100m and no consideration of the pore pressure. H100wPor in Fig.5 means that the calculation is under the condition of CO_2 disposal thickness H=100m and consideration of the pore pressure. The other symbol flags have the similar meaning in our next figures. Fig. 5 shows the shear stress change of fault Case NA under the different disposal thickness (H=100, 150, 200, 250m) of CO_2 bubble with considering the pore pressure. Although with the increase of the injection volume of CO_2 the shear stress accordingly increases whether considering the pore pressure or not, seen from Fig. 4 and Fig. 5, the shear stress change with considering the pore pressure will be obvious, especially at the deep bottom end of the fault.

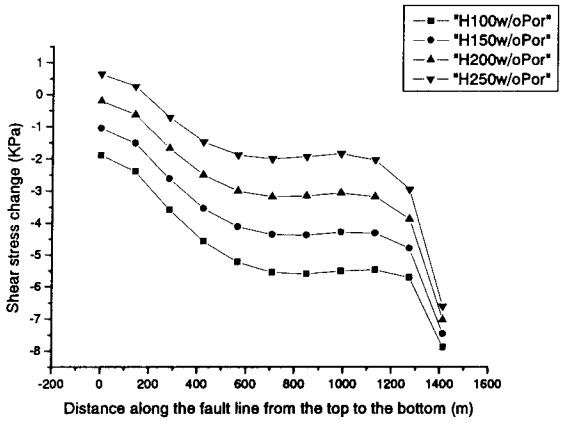

Fig. 4 Shear stress change of fault Case NA with dip angle 45° under the different disposal thickness (H) of CO_2 bubble without considering the pore pressure

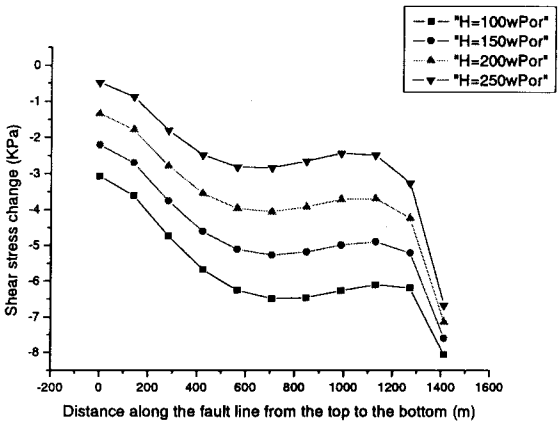

Fig. 5 Shear stress change of fault Case NA with dip angle 45° under the different disposal thickness (H) of CO_2 bubble with considering the pore pressure

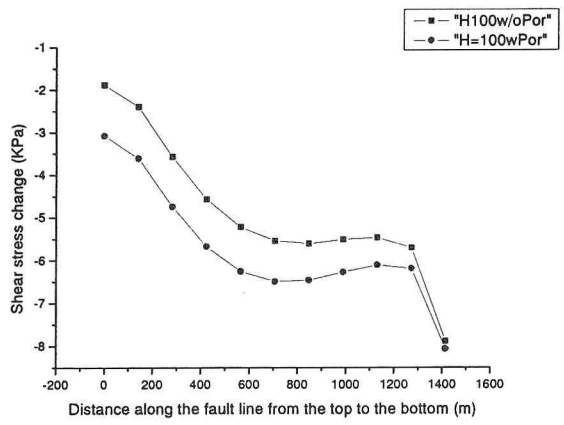

Fig. 6 Shear stress change of fault Case NA with dip angle 45° under the different disposal thickness of CO_2 bubble, H=100

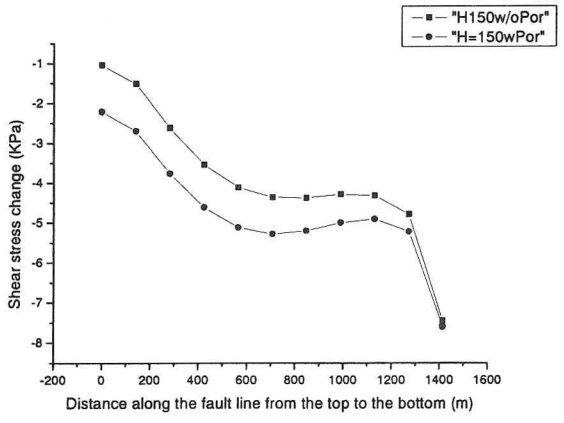

Fig. 7 Shear stress change of fault Case NA with dip angle 45° under the different disposal thickness of CO_2 bubble, H=150

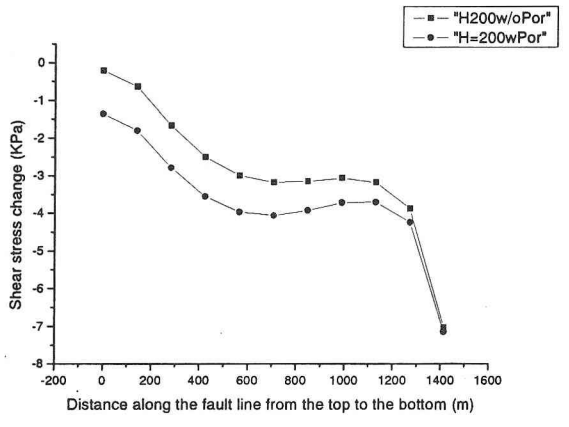

Fig. 8 Shear stress change of fault Case NA with dip angle 45° under the different disposal thickness of CO_2 bubble, H=200

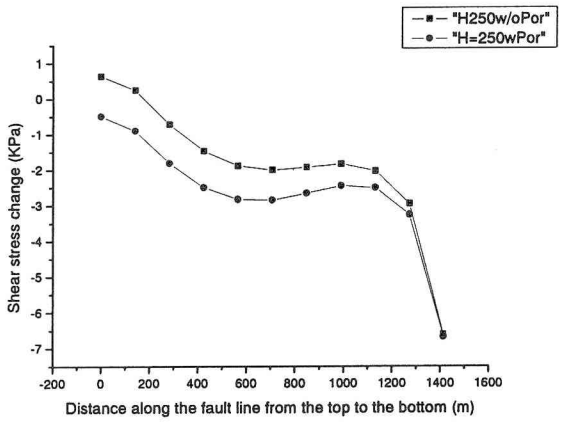

Fig. 9 Shear stress change of fault Case NA with dip angle 45° under the different disposal thickness of CO_2 bubble, H=250

From another viewpoint, Fig.6, Fig. 7, Fig. 8 and Fig. 9 show the comparison of the shear stress change of fault Case NA with or without considering the pore pressure in the numerical model under the different disposal thickness of CO_2 bubble, H form 100m to 250m. Each of them denotes that if consideration of the pore pressure, the shear stress value change of the deep part of the fault will approach one of no considering the pore pressure. With increasing the injection amount of CO_2, this part will extend and the concentration of the pore pressure will be clear over the injected zone, and this concentration phenomenon can be further explained in Fig. 10, Fig. 11, Fig 12 and Fig. 13. The minus value of the shear stress change denotes the normal relative sliding of fault surfaces. In Fig. 10, Fig. 11, Fig 12 and Fig. 13, with increasing the injection amount of CO_2, the pore pressure will accordingly increase, but the value change is relatively small. The concentration of the pore pressure is focused mainly around the injected area and the bottom end of the fault. The negative pore pressure represents the dispersion of the injected zone.

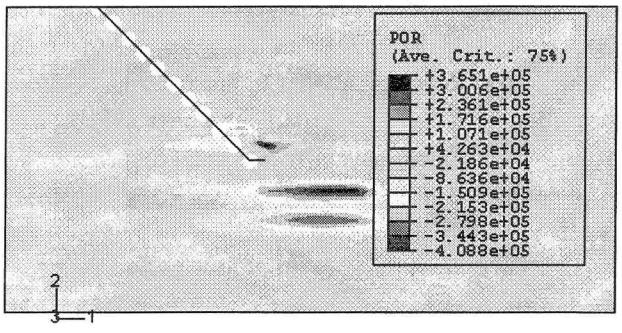

Fig. 10 Contour plot of pore pressure (H=100m)

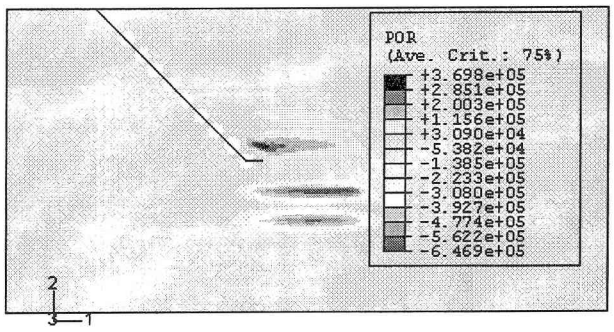

Fig. 11 Contour plot of pore pressure (H=150m)

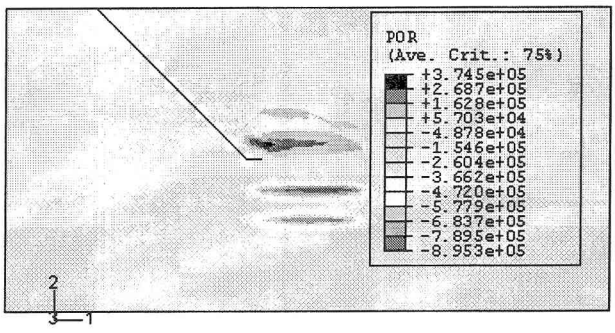

Fig. 12 Contour plot of pore pressure (H=200m)

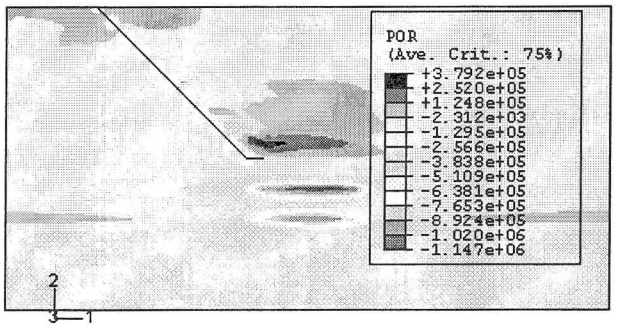

Fig. 13 Contour plot of pore pressure (H=250m)

As the discussion mentioned above, one purpose of our research is to investigate the impact of the pore pressure change induced by the injected CO_2 bubble on the fault during a relatively short geological time so as to determine the stability of faults around the disposal site after injecting a given amount of CO_2 into the geological disposal site. Here, the faults with steep dip angles have been focused in the numerical simulation.

The dip angles of fault case NA varied with three situations, namely 45°, 60° and 75°, are studied. The sketch map is illustrated in Fig. 14. Fig. 15 and Fig. 16 show the shear stress change of fault Case NA with dip angle 60° and 75° under the different disposal thickness (H, from 100m to 250m) of the CO_2 bubble considering the pore pressure in the computational model. From Fig. 5, Fig. 15 and 16, it can be clearly obtained that the shear stress change along the fault is sensitive to the variation of dip angles. For the fault with dip angle 75°, the shear stress change along the fault has very small variation, shown in Fig.16, with increasing the injected amount of CO_2 into deep saline aquifers, but the range of the shear stress value is relatively larger than the other two dip cases. It demonstrates that the fault with a very steep dip angle has weak influence on the variation of the shear stress when the injection volume of CO_2 increases from H=100m to 250m.

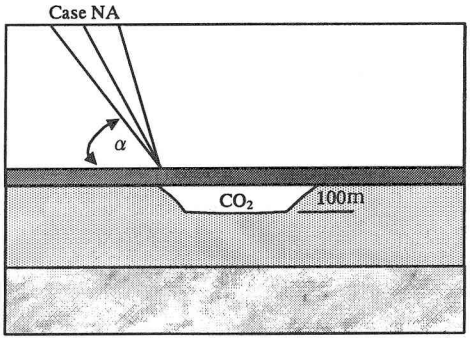

Fig. 14 Sketch map of fault case NA with different dip angles

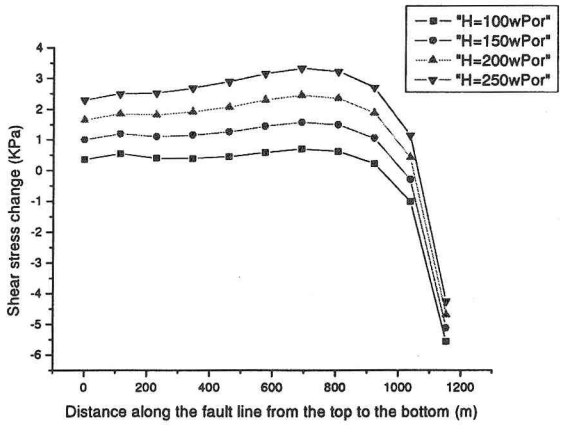

Fig. 15 Shear stress change of fault Case NA with dip angle 60° under the different disposal thickness (H) of CO_2 bubble considering the pore pressure

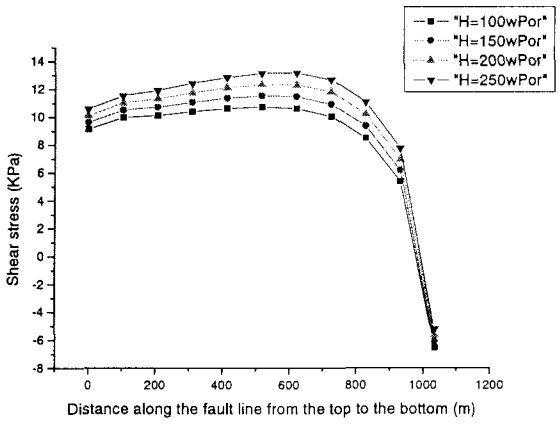

Fig. 16 Shear stress change of fault Case NA with dip angle 75° under the different disposal thickness (H) of CO_2 bubble considering the pore pressure

4.2 Slip Tendency and Safety Factor

From many laboratory experiments, we have observed that increasing pore pressure in rocks and faults reduces their strength and can induce a brittle failure. Fig. 17 illustrates the effects of increasing pore pressure on fault activity. The size of the Mohr circle indicates the differential stress ($\sigma_1 - \sigma_3$), while its position depends on the pore pressure. Increasing pore pressure reduces effective normal stresses and shifts the Mohr circle towards the fault failure envelope. Intersection of the Mohr circle with the failure envelope indicates a fault failure. This usually occurs prior to the failure of relatively strong intact rock that has a failure envelope further to the left. Sliding on a fault due to shear stresses (τ) acting parallel to the fault is resisted by effective normal stresses ($\sigma_n - p_f$) that press opposing fault blocks together (Fig. 18). Sliding occurs on cohesionless faults when the ratio of these stresses equals the coefficient of static friction of the fault

$$\mu = \frac{\tau_{css}}{\sigma_n - p_f}$$

Where τ_{css} is the shear stress that causes a relative sliding, σ_n is the normal stress acting on the fault surfaces, p_f is the pore fluid pressure in the fault, and μ is the coefficient of static friction. The coefficient of static friction is equivalent to the slope of the fault failure envelope in Fig. 17. The shear and normal stress that act on a fault segment are a function of the fault orientation and are given in a two-dimensional form as

$$\tau = \tfrac{1}{2}(\sigma_1 - \sigma_3)\sin 2\theta$$

$$\sigma_n = \tfrac{1}{2}[(\sigma_1 + \sigma_3) - (\sigma_1 - \sigma_3)\cos 2\theta]$$

where σ_1 is the maximum principal stress, σ_3 is the minimum principal stress and θ is the angle between the fault and σ_1 (Fig. 18). The shear and normal stress that act on a fault segment therefore depend on the fault angle θ. Thus, some faults are more favourably oriented for slip than others within a homogeneous stress field. Knowledge of the relative orientation of the stress tensor and faults is hence an essential prerequisite for analyzing the slip tendency of faults.

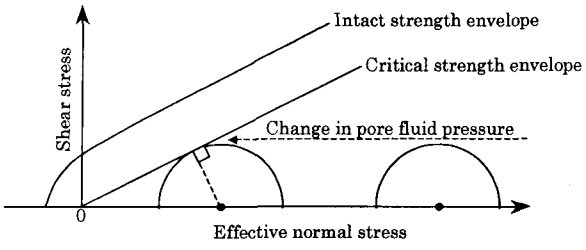

Fig. 17 Effect of increasing pore fluid pressure on fault stability

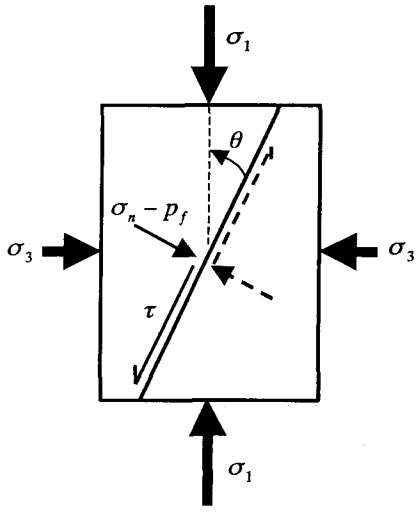

Fig. 18 Stresses resolved on a fault surface

During our analysis, one aim is to determine the slip tendency of faults near or around target disposal areas for CO_2 sequestration. The slip tendency (K_{ts}) may be defined as the ratio of resolved shear stress to normal stress acting on fault surfaces. By also considering the effect of pore fluid pressure, slip tendency is

$$K_{ts} = \frac{\tau}{\sigma_n - p_f}$$

The slip tendency of a cohesionless fault is at a critical level when the resolved stress ratio in the above equation matches the stress ratio required for slip. Generally, the slip tendency is assessed by comparing the ratio of resolved stresses (K_{ts}) with typical friction coefficients for faults. The coefficients of static friction for cohesionless faults typically fall in the range $0.6 \le \mu \le 0.85$ but can be lower if faults contain clay minerals (Jürgen E. Streit and Richard R. Hillis, 2002).

According to the formula discussed above and assuming the frictional parameter 0.6 of the fault surfaces, the slip tendency of the fault in our geomechanical model can be calculated. Fig. 19 draws out the variation of slip tendency of the fault with the increase of CO_2 disposal thickness. In Fig. 19, wPor implies that the pore pressure is considered in our geomechanical model, and w/oPor means that the pore pressure is not considered. This figure clearly shows us that when the pore pressure is considered the factor of slip tendency will increase. Regardless of considering the pore pressure or not, the slip tendency factor will increase accordingly with the enlargement of CO_2 disposal thickness.

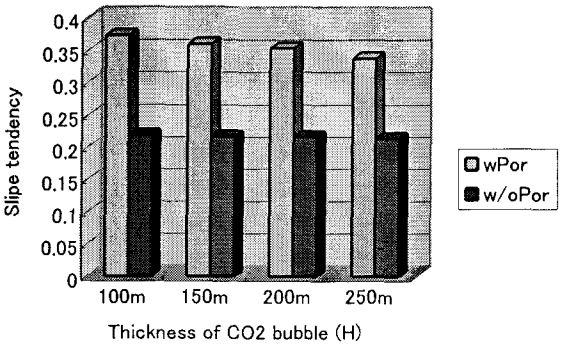

Fig. 19 Relationship between slip tendency and size CO_2 disposal thickness

As we have known, the Mohr-Coulomb failure criterion is often adopted in geotechnical engineering analysis. The slip tendency factor just discussed above is also deduced in the Mohr circle space. In our research, we consider the safety factor used in the practical engineering from another viewpoint. A value close to the failure level, as shown in Fig. 20, is adopted as the local safety factor, F_s, and it is used to evaluate the stability of the faults with no considering the effects of pore pressure directly in this formula. Table 3 lists the local safety factor of faults (H=100m), Case NA and Case FB, which are analyzed according to three different dip angles, 30°, 45° and 60°, in our research. Viewing from Fig. 21, the following two trends can be found: (1) with faults being far away from the disposal zone, the value of the safety factor will increase. (2) the steep dip faults easily get the high value of the safety factor. This is an important factor to evaluate the obvious influence of CO_2 sequestration on the geomechanical system.

From the derivation of the slip tendency and the local safety factor, we found that in the assessment of the final stage both of them should be considered at the same time in order to fully grasp the effects of the pore pressure in the whole geomechanical system, because the slip tendency can directly consider the pore pressure in the formula, but the local safety factor is much more common in engineering assessment.

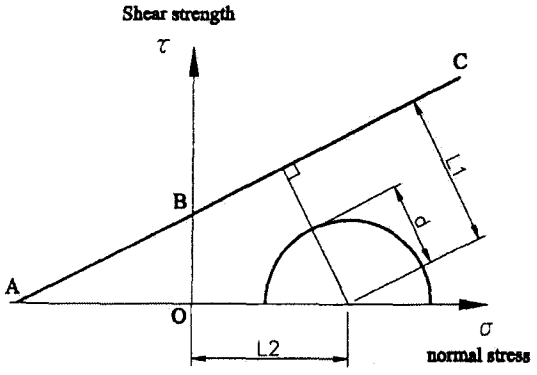

Fig. 20 Definition of the local safety factor

4. Conclusions

In this paper, finite element models with elastic material properties both in the continuous body and on the fault surfaces are used to simulate the influence of the pore pressure induced by the injected CO_2 driven buoyancy on the disposal system, especially effects on

the fault surfaces, after the captured CO_2 is injected into the deep saline aquifers for a relatively short geological time. From our research discussed above, three suggesting conclusions are followed:

Table 3 Comparison of the safety factor of different faults

Fault Cases		F_s
Case NA	$\alpha = 30^\circ$	1.012
	$\alpha = 45^\circ$	1.195
	$\alpha = 60^\circ$	1.254
Case FB	$\alpha = 30^\circ$	1.220
	$\alpha = 45^\circ$	1.433
	$\alpha = 60^\circ$	1.660

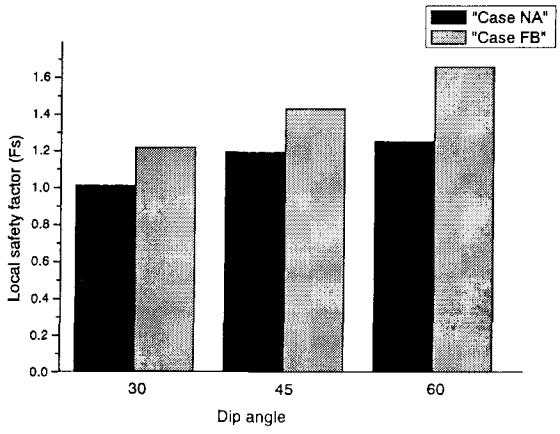

Fig.21 The local safety factor of faults with different dip angles

(1) The pore pressure has obvious influence on the fault behavior in the geomechanical system of CO_2 sequestration. The shear stress change of fault surfaces induced by the pore pressure is clear, especially at the deep bottom end of the faults.

(2) The effects of the pore pressure on the fault surfaces are sensitive to the dip angles of the faults. The fault with a very steep dip angle has weak influence on the variation of the shear stress when the CO_2 disposal thickness increases from H=100m to 250m.

(3) Although the slip tendency and the local safety factor can be used to evaluate the stability of the faults, both of them should be considered at the same time in the geomechanical sequestration system in order to roundly consider the pore pressure in formations.

References

1) ABAQUS/Standard User's Manual 6.2, H. K. S. Inc., USA, 2001

2) Jürgen E. Streit and Richard R. Hillis, Building geomechanical models for the safe underground storage of carbon dioxide in porous rock, in J. Gale and Y. Kaya Eds., *Greenhouse Gas Control Technologies (GHGT-6)*, Pergamon Publishing, pp.495-500, 2002

3) Kaya, Y., Koide, H., Nakaya, S., Ohsumi, T., Takita, K., Yoshimura, H., Underground sequestration of carbon dioxide in tectonically active area, *Greenhouse Gas Control Technologies*, pp. 296-298,1999

4) Koide, H., Shindo, Y., Tazaki, Y., Iijima, M., Ito., K., Kimura, N. and Omata, K., Deep Sub-seabed Disposal of CO_2 – The Most Protective Storage, *Energy Conversion and Management*, 38, pp. 253-258, 1997

5) Li, Q., Wu, Z. S., Li, X. C., Ohsumi, T. and Koide, H., Numerical simulation on crust deformation due to CO_2 sequestration in deep aquifers, *Journal of Applied Mechanics*, Vol.5, pp.591-600, 2002

6) Li, Q., Wu, Z. S., Li, X., Ohsumi, T. and Koide, H., Fault stability behavior due to geological sequestration of CO_2, *Journal of Structural Engineering, AIJ*, Vol.50B, pp.497-504, March, 2004.

7) OECD/NEA, Review of Safety Assessment Methods, A Report of the Performance Assessment Advisory Group of the Radioactive Waste Management Committee, OECD Nuclear Energy Agency, 1991

(Received: April 16, 2004)